electron jumps from the ground to first excited state with the probability per unit time f_b.

Thus, one can write

$$\langle \Delta\omega_0^1(t_1)\ \Delta\omega_0^1(t_2)\rangle = \sum_{j,k} \Pi(j/k)\ \Delta\omega_0^1(j)\ \Delta\omega_0^1(k)\ P_0(\Delta\omega_0^1(k)) \tag{B4}$$

where $P_0(\Delta\omega_0^1(k))$ is the initial distribution of the angular speed. The initial distribution is taken as

$$P_0(\Delta\omega_0^1(k)) = \delta(\Delta\omega_0^1(k) - b) \tag{B5}$$

and

$$\langle \Delta\omega_0^1(t_1)\ \Delta\omega_0^1(t_2)\rangle = \Pi(2/1)\ \Delta\omega_0^1(2)\ \Delta\omega_0^1(1) + \Pi(1/1)\ \Delta\omega_0^1(1)\ \Delta\omega_0^1(1) \tag{B6}$$

where $\Pi(2/1)$ is the conditional probability that at $t = t_1 - t_2$ the electron jumps from the ground state to its first excited state. The conditional probability $\Pi(j/k)$ is governed by (B2). Solving the master equation, we have

$$\Pi(l/k) = \sum_m C_{lm}[\exp(w_{mm}t)]\tilde{C}_{mk} \tag{B7}$$

where

$$\mathbf{w} = \tilde{\mathbf{c}}\mathbf{W}\mathbf{c} = \begin{pmatrix} -f_b & 0 \\ 0 & 0 \end{pmatrix} \tag{B8}$$

and

$$\mathbf{c} = \frac{1}{\sqrt{2}}\begin{pmatrix} 1 & -1 \\ -1 & -1 \end{pmatrix} \tag{B9}$$

Then, substituting (B7) into (B6), we obtain

$$\langle \Delta\omega_0^1\ \Delta\omega_0^1(t_2)\rangle = b^2 \exp[-f_b(t_1 - t_2)] \tag{B10}$$

Absorption Spectrum of the Solvated Electron. 2. Numerical Calculations of the Profiles of the Electron in Water and Methanol at 300 K

Halina Abramczyk and Jerzy Kroh*

Institute of Applied Radiation Chemistry, Technical University, 93-590 Lodz, Wroblewskiego 15, Poland
(Received: May 17, 1990)

The absorption band profiles of the solvated electrons in the spectral range 0.62-2.48 eV were calculated in terms of the theory presented in our previous paper. We considered the influence of the environment, the effect of fluctuations of the energy potential shape, and the band profiles as a function of the coupling strength with intramolecular vibrations of the solvent. The theory gives good agreement with experiment for the electron solvated in water and alcohols at 300 K.

1. Introduction

The absorption spectra of solvated electrons in liquids and glasses are characterized by the position of the band maximum and the characteristic band shape. Experimentally, almost all solvated electron spectra are broad 0.4-1.86 eV and skewed to the high-energy side, displaying little or no vibrational structure. One of the most interesting results of the time-resolved and stationary measurements at low temperatures is the detection of an absorption band of the solvated electron in the near-infrared spectral range for many liquids and glasses. This problem has received much attention in literature.[1-8] The first major theoretical problem is how to explain the exceptional width of the absorption band.

Most of the theoretical models[7-11] predict a line shape that is too narrow and symmetric compared to experiment. Some of them[13-17] claim successful fits. A second related problem is how to understand the physical reason for the existence of the IR-absorbing electrons (e^-_{IR}). Any successful theory should be able to explain all of these characteristics of the absorption spectrum. In the previous paper[19] we proposed a theoretical model that takes into account the following mechanisms as the dominant broadening factors: anharmonic coupling of the solvated electron to intramolecular vibrational modes of the solvent, inhomogeneous broadening due to the molecular motion, and nonlocalized transitions due to the electron tunneling.

The purpose of the present paper is to examine to what extent the experimental band shapes of solvated electrons in the visible region can be understood in terms of the theory presented in our previous paper[19] and which of the above-mentioned mechanisms gives a dominant contribution to the band broadening. In a further paper we will concentrate on the spectrum in the near-infrared region.

2. Numerical Calculations of the Absorption Band Shape

In the framework of the linear response theory the absorption coefficient is expressed as

$$\epsilon(\omega) = \frac{2\pi\omega}{3\hbar cnV}(1 - \exp(-\beta\hbar\omega))\int_{-\infty}^{+\infty} \langle M^+(t)\ M(0)\rangle e^{-i\omega t}\, dt \tag{1}$$

where M denotes the dipole moment of the sample, V its volume, and n the refractive index. We have calculated[19] that the dipole

(1) Hase, H.; Noda, M.; Higashimura, T. *J. Chem. Phys.* **1971**, *54*, 2975.
(2) Baxendale, J. H.; Sharpe, P. H. G. *Chem. Phys. Lett.* **1976**, *39*, 401.
(3) Klassen, N. V.; Gillis, H. A.; Teather, G. G.; Kevan, L. *J. Chem. Phys.* **1975**, *62*, 2474.
(4) Ogasawara, M.; Shimizu, K.; Yoshida, K.; Korh, J.; Yoshida, H. *Chem. Phys. Lett.* **1979**, *64*, 43.
(5) Kevan, L. *J. Chem. Phys.* **1972**, *56*, 838.
(6) Shida, T.; Iwata, S.; Watanabe, T. *J. Phys. Chem.* **1972**, *76*, 3683.
(7) Bush, R. L.; Funabashi, K. *J. Chem. Soc., Faraday Trans. 2* **1977**, *73*, 274.
(8) Okazaki, K.; Freeman, G. R. *Can. J. Chem.* **1978**, *56*, 2313.
(9) Gaathon, A.; Jortner, J. *Electrons in Fluids*; Jortner, J., Kestner, N. R., Eds.; Springer-Verlag: New York, 1973; p 429.
(10) Webster, B. C.; Carmichael, I. *J. Chem. Phys.* **1978**, *68*, 4086.
(11) Kestner, N. R. In *Electron-Solvent and Anion Solvent Interactions*; Kevan, L., Webster, B., Eds.; Elsevier: Amsterdam, 1976; Chapter 1.
(12) Tachiya, M.; Tabata, Y.; Oshima, K. *J. Phys. Chem.* **1973**, *77*, 263.
(13) Kajiwara, K.; Funabashi, K.; Naleway, C. *Phys. Rev. A* **1972**, *6*, 808.
(14) Huang, J. T.; Ellison, F. O. *Chem. Phys. Lett.* **1974**, *28*, 189.
(15) Mezzacurati, V.; Signorelli, G. *Lett. Nuovo Cimento* **1975**, *12*, 347.
(16) Banerjee, A.; Simons, J. *J. Chem. Phys.* **1978**, *68*, 415.
(17) Bartczak, W. M.; Hilczer, M.; Kroh, J. *J. Phys. Chem.* **1987**, *91*, 3834.
(18) Rossky, P. J.; Schnitker, J. *J. Phys. Chem.* **1988**, *92*, 4277.
(19) Abramczyk, H. *J. Phys. Chem.*, preceding paper in this issue.

0022-3654/91/2095-6155$02.50/0

correlation function $\langle M^+(t)\, M(0)\rangle$ is given by

$$G(t,P) = \langle M^+(t)\, M(0)\rangle = e^2\epsilon\epsilon_1 \sum_{\gamma=0}^{\infty} \epsilon_2(\gamma) \sum_{m=1}^{4} \{ \sum_{\alpha=0}^{\gamma} \sum_{j=0}^{\alpha} \sum_{k=0}^{\alpha} \sum_{l=0}^{\infty} \sum_{p=0}^{l} A_{lp\gamma\alpha j} C_{kjl\gamma\alpha} \langle B^m_{\gamma\alpha}\rangle \} + \sum_{\alpha=\gamma+1}^{\infty} \sum_{j=0}^{\gamma} \sum_{k=0}^{\gamma} \sum_{l=0}^{\infty} \sum_{p=0}^{l} A_{lp\alpha\gamma j} C_{kj\alpha\gamma} \langle B^m_{\alpha\gamma}\rangle \quad (2)$$

where

$$A_{lp\gamma\alpha j} = \binom{l}{p} \frac{\gamma!\alpha!(-1)^{k+j+l}}{2^l(\alpha-k)!(\alpha-j)!(\gamma-\alpha+k)!(\gamma-\alpha+j)!} \quad (3)$$

$$C_{kjl\gamma\alpha} = {\alpha_0}^{2(k+j+l+\gamma-\alpha)} \quad (4)$$

$$\langle B^m_{\gamma\alpha}\rangle = f_m \exp\{-i[\langle\omega_0^l\rangle + \langle\omega^{mt}\rangle - 2{\alpha_0}^2\omega_{00} + (\gamma-\alpha)\omega_{00}t]\} \times \exp\{-[(\gamma-\alpha) + 2p + 2j]\Gamma t/2\} \exp\{-2a^2[\tau_a{}^2(\exp(-t/\tau_a) - 1) + \tau_a t]\} \exp\{-b^2[\tau_b{}^2(\exp(-t/\tau_b) - 1) + \tau_b t]\} \quad (5)$$

All of the other symbols in eqs 2–5 have been explained in ref 19.

The correlation function $G(t,P)$ depends in our model on the following molecular properties P: $\langle\omega_0^l\rangle$, ω_{00}, α_0, Γ, τ_a, τ_b, a, and b. The angular speed $\langle\omega_0^l\rangle$ denotes the electronic transition of the solvated electron, when there is no coupling to the intramolecular vibrational degrees of freedom of the solvent. It can be treated as the depth of the electron trap. The angular speed ω_{00} is the frequency of the normal mode of the solvent molecule that is coupled to the electron. The anharmonic coupling constant α_0 reflects the strength of this coupling, whereas the damping parameter Γ reflects the strength of the coupling between the mode ω_{00} and the thermal bath (translational, reorientational, low-frequency intermolecular vibrations). The parameter Γ describes the influence of the environment on the absorption spectrum of the solvated electron exerted indirectly through the ω_{00} mode. In fact, however, the environment interacts with the electron also directly through the long-range Coulombic interactions. This effect enters into our model through the parameter a, which is the average value of the energy jump of the energy levels caused by the fluctuations of the potential well due to the molecular motions of the solvent. Both Γ and a are of the order of thermal energy kT. The time scale of the fluctuations for the equilibrated traps is characterized by the correlation time τ_a, which is the inverse of the probability per unit time of making the jump a. It reflects the time scale of the molecular motion of the solvent, especially reorientational motion. Thus, we can treat it as a reorientational correlation time τ_1 or τ_2 (depending on the physical nature of the electron–vibron coupling) which can be experimentally obtained from dielectric relaxation, IR or T_1 NMR measurements, and Raman line-shape analysis.[20] Taking into account the different time scale of the molecular motion and the electronic transitions, the time fluctuations from the environment can be regarded as a static case in terms of the classification of the linear response theory.[21] There is another factor, may be much more important, resulting in the fluctuations with time of the energy levels of the potential well. It is well-known that during an electronic transition the positions and the velocities of all atomic nuclei forming the trap remain constant (Franck–Condon principle) and its electronic charge distribution is altered. Because of the change in the electronic structure of the trap the electronic transition occurs between the energy surfaces characterized by different equilibrium geometries. This causes the well-known shift of the electronic phase angular speed according to the rule

$$\omega_{\tau\alpha} = \langle\omega_0^l\rangle - 2{\alpha_0}^2\omega_{00} + (\gamma-\alpha)\omega_{00} \quad (6)$$

which gives rise to a progression of vibrational peaks separated by the values of ω_{00} of the vibrational mode. However, such transition contributes also to the band broadening as we have shown recently.[19] Indeed, the electronic transition between the energy surfaces characterized by different equilibrium geometries can be regarded as the transition in the same potential well, fluctuating in time. The time scale of the fluctuations is characterized by the correlation time $\tau_b = \langle\omega_0^l\rangle^{-1}$ whereas the average value of the fluctuations is given by b. As we can see from the above discussion, the parameters $\langle\omega_0^l\rangle$, α_0, and b are adjustable ones in our model. All of the others can be obtained from experiment (ω_{00}, τ_a, τ_b) or reasonably estimated (Γ, a). The factors f_m in eq 5 provide the information about the transition matrix elements $\langle n|r|m\rangle$ and depend on the average static potential well in which the electron motion occurs. They can be obtained from ab initio SCF or model calculations. Here, we have used harmonic approximation with

$$f_1 = {r_{01}}^2 = \hbar/2m\langle\omega_0^l\rangle \quad (7)$$

where m is the electron mass.

We tested our model for the assumption that the electron motion occurs in a single minimum potential well. It means that there is no tunneling and $f_m = 0$ (except f_1), $\langle\omega^{mt}\rangle = 0$ and $a = 0.0$.

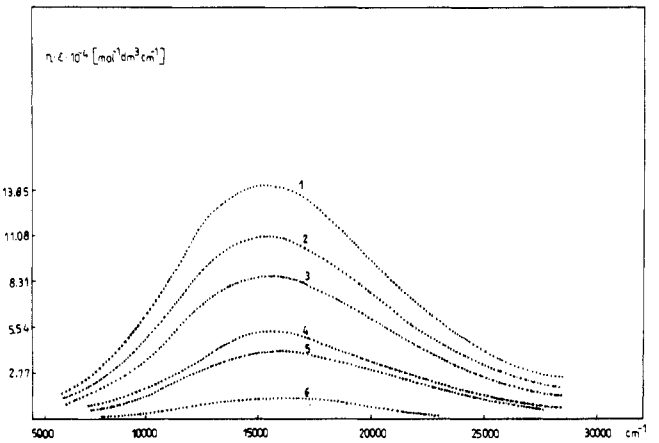

Figure 1. Absorption coefficient ϵ as a function of the anharmonic coupling constant α_0, $\langle\omega_0^l\rangle = 24\,000$ cm^{-1} (2.975 eV), $\omega_{00} = 1345$ cm^{-1} (0.167 eV), $\Gamma = 300$ cm^{-1} (0.037 eV), $a = 0.0$, $b = 0.0$; (1) $\alpha_0 = 2.60$, (2) $\alpha_0 = 2.58$, (3) $\alpha_0 = 2.56$, (4) $\alpha_0 = 2.52$, (5) $\alpha_0 = 2.50$, (6) $\alpha_0 = 2.40$.

3. Results and Discussion

The results of the numerical calculations according to eqs 1 and 2 are presented here. First, for illustrative purposes, we have shown the interplay between the various factors, which affect the band shape. In Figure 1 we have shown the profiles as a function of the anharmonic coupling constant α_0 for a reasonable set of the other parameters given in the description of the figure. An inspection of the Figure 1 shows that the absorption coefficient increases considerably, whereas its maximum position is slowly shifted toward lower frequencies, when the coupling constant increases. With increasing α_0, the profiles become distinctly asymmetric with a slope steeper at the low-frequency side. The coupling electron–vibron characterized by α_0 depends on the short-range interactions. However, it can strongly be modified by the molecular geometry of the trap, which depends generally both on short- and long-range interactions. If, for example, in alcohols, electron was localized in the hydroxyl group trap, the coupling with the modes associated with OH would be much stronger than that with the alkyl moieties. The results presented in Figure 1 have been calculated for the static potential well ($b = 0$). In Figure 2 we have shown the effect of the fluctuations of the potential well on the band shape. We can see that the fluctuations lead to smoothing of the band profiles. It may be one of the reasons that the absorption bands of the solvated electron display little or no vibrational substructure. In order to investigate the question concerning the effect of the environment the absorption profiles as a function of the damping parameter Γ were calculated.

If we considered that the electron being localized only due to the coupling electron–vibron was isolated from their environment

(20) Berne, B. J. *Physical Chemistry*; Academic Press: New York, 1971; Vol. VIIIB.

(21) Kubo, R. *J. Phys. Soc. Jpn.* **1962**, *17*, 1100.

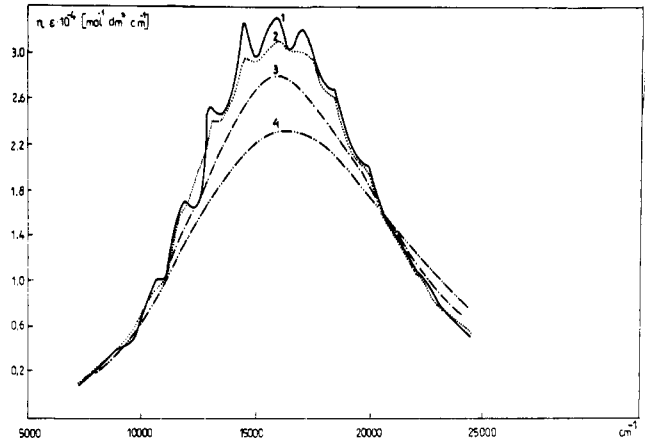

Figure 2. Influence of the fluctuations of the potential well on the absorption coefficient ϵ, $\langle\omega_0^1\rangle$ = 24 000 cm^{-1} (2.975 eV), ω_{00} = 1345 cm^{-1} (0.167 eV), Γ = 100 cm^{-1} (0.012 eV), a = 0.0, α_0 = −2.46; (1) b = 0.0, (2) b = 1000 cm^{-1} (0.124 eV), (3) b = 2000 cm^{-1} (0.025 eV), (4) b = 3000 cm^{-1} (0.372 eV).

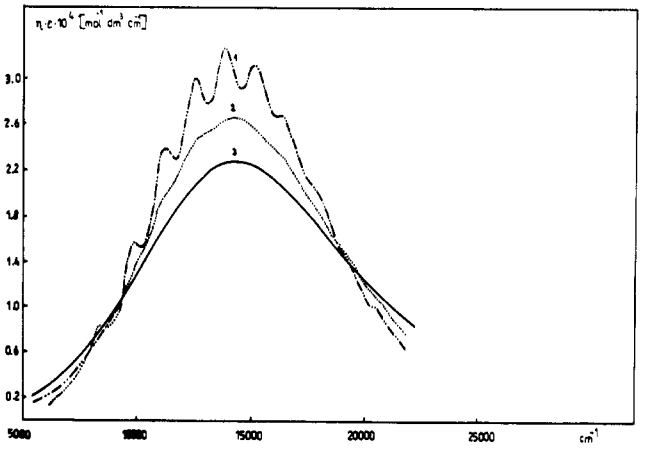

Figure 3. Absorption coefficient ϵ as a function of the damping parameter Γ, $\langle\omega_0^1\rangle$ = 22 000 cm^{-1} (2.727 eV), ω_{00} = 1345 cm^{-1} (0.167 eV), α_0 = −2.52; (1) Γ = 100 cm^{-1} (0.012 eV), (2) Γ = 200 cm^{-1} (0.025 eV), (3) Γ = 300 cm^{-1} (0.037 eV).

(trap), the spectrum would consist of a set of δ function peaks with a distribution of intensities corresponding to the Franck–Condon factors and Γ would be equal to zero. When Γ increases, the influence of the environment on the band shape becomes important as we can see in Figure 3. The absorption band loses its vibrational structure. So, it means that the environment and the fluctuations of the potential well lead to the similar effect on the band shape. In Figure 4 we have shown the effect of the depth of the trap on the band profile. As expected, the maximum position is progressively shifted to low frequencies with decreasing of the trap depth.

To illustrate how our model works for realistic systems we will concentrate on the most frequently studied system as the electron solvated in water and alcohols. The solvated electron in H_2O exhibits an intense optical absorption band in the visible region with a peak at 1.73 eV at 25 °C[22] and the band width $W_{1/2}$ 0.843 eV.[23] In D_2O the spectrum is blue-shifted[24,25] and have $W_{1/2}$ equal to 0.802 eV.[23] The value of the $W_{1/2}$ in alcohols is nearly double that in water. The asymmetry of the band is also larger in alcohols than in water.[23] The band peak is observed at 1.95 eV in methanol and at 1.79 eV in ethanol at 300 K.[23] We must turn for a moment to the parameters, which have been used for calculation of the

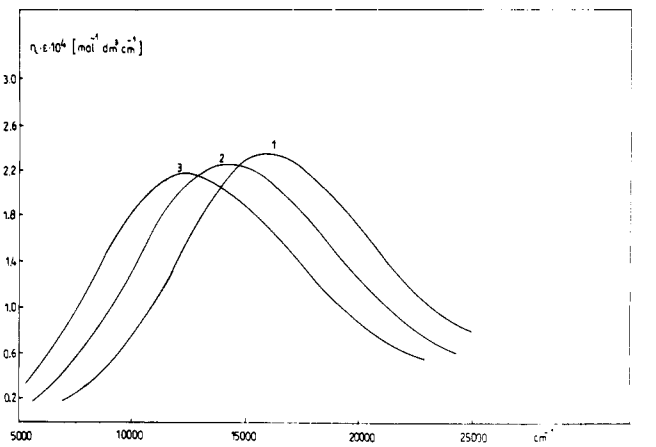

Figure 4. Absorption coefficient ϵ as a function of the depth of the electron trap $\langle\omega_0^1\rangle$, ω_{00} = 1345 cm^{-1} (0.167 eV), Γ = 300 cm^{-1} (0.037 eV), α_0 = −2.46, a = 0.0, b = 0.0; (1) $\langle\omega_0^1\rangle$ = 24 000 cm^{-1} (2.976 eV), (2) $\langle\omega_0^1\rangle$ = 22 000 cm^{-1} (2.727 eV), (3) $\langle\omega_0^1\rangle$ = 20 000 cm^{-1} (2.479 eV).

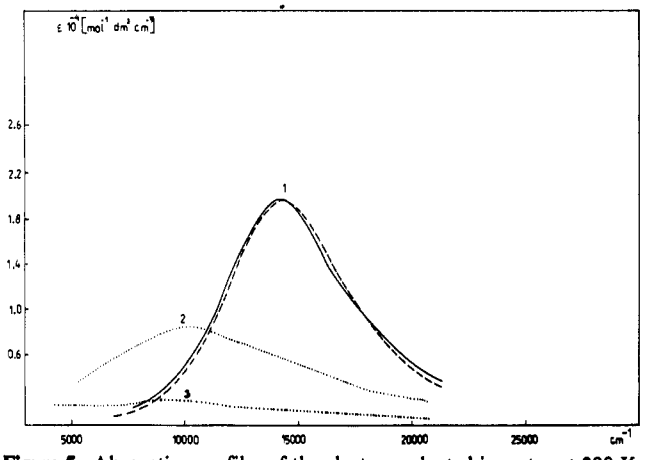

Figure 5. Absorption profiles of the electron solvated in water at 298 K: (---) theory, (—) experiment,[23] $\langle\omega_0^1\rangle$ = 185 000 cm^{-1} (2.29 eV), Γ = 212 cm^{-1} (0.026 eV), α_0 = −2.42, a = 0.0, b = 0.0, n = 1.332; (1) ω_{00} = 710 cm^{-1} (0.088 eV) (ν_t), (2) ω_{00} = 1595 cm^{-1} (0.197 eV) (ν_b), (3) ω_{00} = 3600 cm^{-1} (0.446 eV) (ν_S).

theoretical absorption spectrum. First, let us discuss the influence of the normal modes ω_{00}. Water has three normal modes: stretching symmetric ν_S at 3651 cm^{-1} (0.452 eV), stretching asymmetric ν_{AS} at 3755.8 cm^{-1} (0.465 eV), and bending ν_b at 1595 cm^{-1} (0.197 eV)[26] in the vapor phase. The vibrational modes are significantly disturbed by H-bond formations. The stretching mode ν_S is shifted to lower frequencies by 310 cm^{-1} whereas the bending mode shifts upward by 10–15 cm^{-1} upon H-bond formation.[27] The formation of H bond restricts certain rotational and translational degrees creating a new vibration degrees of freedom. One of them is vibration of torsional type ν_t at 710 cm^{-1} (0.088 eV) for water.[28] In Figure 5 we have shown the calculated absorption spectra of the solvated electron in water for the coupling with all of the normal modes. The damping parameter was put as 212 cm^{-1} (0.026 eV) for H_2O corresponding to the stretching mode ν_g of the hydrogen bridge OH···O.[28] Indeed, it is well-known[29,30] that the coupling between the stretching modes ν_S and ν_σ is dominant in solvents forming H bond compared with all of the other intermolecular low-frequency modes of the solvent. In addition, the other characteristic low frequencies, i.e., 175 cm^{-1}

(22) Hart, E. J.; Anbar, M. *The Hydrated Electron*; Wiley-Interscience: New York, 1970.
(23) Jou, F. Y.; Freeman, G. R. *J. Phys. Chem.* **1977**, *81*, 909.
(24) Michael, B. D.; Hart, E. J.; Schmidt, K. H. *J. Phys. Chem.* **1975**, *80*, 2798.
(25) Brown, D. M.; Dainton, F. S.; Keene, J. P.; Walker, D. C. *Proc. Chem. Soc.* **1964**, 266.
(26) Luck, W. A. P. In *Structure of Water and Aqueous Solutions*; Luck, W. A. P., Ed.; Verlag Chemie: Weinheim, FRG, 1974; p 220.
(27) Greinacher, E.; Luttke, W.; Mecke, R. *Z. Elektrochem.* **1955**, *59*, 23.
(28) Giguere, P. A.; Harvey, K. B. *Can. J. Chem.* **1956**, *34*, 798.
(29) Pimental, G. C.; McClellan, A. L. *The Hydrogen Bond*; Freeman: San Francisco, 1960.
(30) Schuster, P.; Zundel, G.; Sandorfy, C. *The Hydrogen Bond*; North-Holland: Amsterdam, 1976.

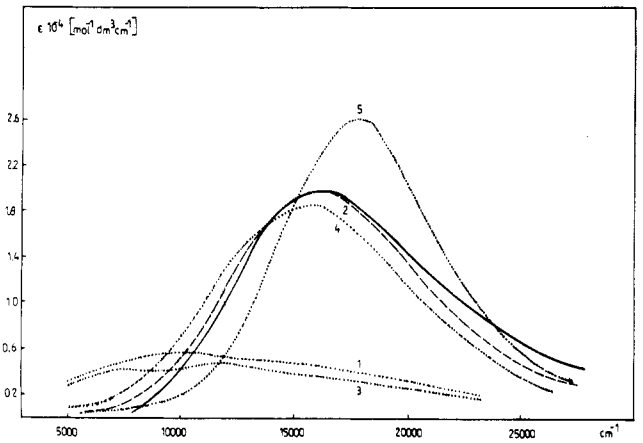

Figure 6. Absorption profiles of the electron solvated in methanol at 198 K (---) theory, (—) experiment,[23] $\langle\omega_0^1\rangle$ = 24 000 cm^{-1} (2.976 eV), Γ = 222 cm^{-1} (0.027 eV), $\alpha_0 = -2.46$, $a = 0.0$, $b = 0.0$, $n = 1.33$; (1) ω_{00} = 3679 cm^{-1} (0.456 eV) (ν_S), (2) ω_{00} = 1345 cm^{-1} (0.167 eV) (ν_b), (3) ω_{00} = 3000 cm^{-1} (0.372 eV), (4) ω_{00} = 1450 cm^{-1} (0.179 eV), (5) ω_{00} = 1050 cm^{-1} (0.130 eV).

(0.0216 eV), for H_2O associated with translational mode are close to the frequency ν_σ values and would give similar effect. The bending mode ν_β at 50 cm^{-1} are known to be weakly coupled to H-bond normal modes and can be neglected. We can see from Figure 5 that the experimental band of water is well reproduced only if we assume the coupling between electron and the torsional mode ν_t. The coupling with ν_b gives doubled and with ν_S 3 times broader bandwidth as compared with experiment and rather too deep trap taking into account ab initio[31] and model[32] calculations. The same discussion can be repeated for methanol. The normal modes of methanol[33] can be divided into five groups of frequency ranges (1) stretching mode ν_S(OH) at 3679 cm^{-1} (0.456 eV) (shifted to 3525 cm^{-1} (0.437 eV) upon H bond[33]), (2) bending mode ν_b at 1345 cm^{-1} (0.166 eV), (3) stretching modes of the CH bonds in the range 2800–3000 cm^{-1} (3000 cm^{-1}), 0.372 eV), (4) CH deformation modes in the range 1420–1480 cm^{-1} (1450 cm^{-1}, 0.179 eV), (5) CO stretching and CH rocking modes in the range 1030–1070 cm^{-1} (1050 cm^{-1}, 0.130 eV).

The numbers taken for calculations are given in parentheses. The OH···O stretching mode ν_σ is observed at 222 cm^{-1} (0.027 eV)[35] and this number is put as Γ. The results are given in Figure 6. As we can see, the coupling with the stretching modes of the OH and CH groups gives negligible contribution to the experimental profile $\epsilon(\omega)$. On the other hand, reproducing the band maximum by parametrizing $\langle\omega_0^1\rangle$ for ν_S or CH stretching gives an unreasonably broad bandwidth. An inspection of Figure 6 indicates that it is hard to distinguish which of vibrational modes belonging to the groups 2, 4, and 5 give the dominant contribution to the band shape. However, the coupling with ν_b in the hydroxyl trap excludes the coupling with CH deformation and rocking modes in the alkyl trap due to the steric reasons. Taking into account the depth of the trap in the theoretical bands (2.97 eV); which is greater than in water (2.35 eV), it is rather impossible to expect that this trap is formed from the alkyl groups. The best agreement with experiment is obtained for the coupling of electron with the bending mode ν_b. Only the coupling with ν_b gives the right asymmetry of the band. The coupling with CO stretching gives the symmetric band. However, it seems that contribution from the CO mode on the high-energy side to the spectrum cannot be excluded.

The question arises as to why the electron is mainly coupled in water with the torsional mode ν_t, whereas in methanol with the bending mode ν_b. This may be related to two contrasting geometries of solvated electrons in water and methanol suggested by Kevan as OH oriented and dipole oriented.[31] The structures obtained from the interpretation of the experimental ESEM results[36,37] are such that in water the electron is surrounded by six molecules arranged with one OH bond of each water oriented octahedrally about electron with an electron to proton distance of 2.1 Å. In ethanol the electron is surrounded tetrahedrally by four ethanols arranged with their molecular dipoles, which approximately bisect the COH bond angle, oriented toward the electron. Although the validity of Kevan's interpretations has been questioned in a few papers,[38] it seems that there are more arguments in favor of the OH oriented for water and dipole oriented for alcohols.[18,39-41]

It is clear that the geometry with the hydrogen bond oriented toward the electron must be modified by the vibrations sensitive to the H-bond formation. It is well-known that the spectral changes in ν_t caused by the H bond are much more spectacular than those occurring for ν_b. In the geometry with molecular dipoles oriented toward electron, the bending mode modifies the angle COH in alcohols and changes in this way the direction of the dipole moment. In both cases there is no need to assume that tunneling modifies the band profile. It means that the short-time dynamics probed by the spectral band shape is not affected by tunneling.

It is of interest to compare, as far as possible, the calculated spectra with the results presented in the other papers. Kajiwara et al.[13] and Bush and Funabashi[7] simulated the band shape for the solvated electron in water and alcohols. Kajiwara et al.[13] proposed a modified cluster model treating the bound electron as a particle in a box with the size and the depth of the trap as parameters. The parameters are chosen in such way it has only one bound state and the theoretical spectrum is assigned to a bound to continuum transition. The spectra for water obtained in this way agree well with the experimental line shape. The small-polaron model[7] for alcohols also assumes that only continuum excited states of the anion exist and the electron is coupled to the bending mode ν_b, which is in agreement with our conclusions. Although the polaron model predicts the transition energies corresponding to absorption maxima with reasonable choice of parameters, the broadness and asymmetry of the spectral profile could not be explained without introducing additional parameters such as a distribution of the trap size. The models built on the assumption of the continuum excited state are not justifiable for alcohols and water in light of the photoconductivity results.[42] Recently, Bartczak et al.[17] fit satisfactorily the experimental spectrum of the electron in water. The calculations are based on the assumption of the statistical variety of electron traps in disordered media. However, the estimation of the distribution function $p(h)$ characterizing the structural parameters of the trap on the basis of the rotational bands of the IR spectrum has to be doubted. The optical spectrum for electron in water[18] obtained by a path-integral simulation reproduces the exceptional breadth and the asymmetry. However, the maximum of the band is not predicted, showing the shift to higher energy by 0.7 eV. They suppose that this effect is attributed to the approximate nature of the electron–solvent pseudopotential. We think that there is a reason for this discrepancy other than the inadequacy of the potential they have used. They have performed calculations of the spectrum by solving the Schrodinger equation for one electron interacting with rigid water molecules within the Born–Oppenheimer approximation, so the coupling of the electron to molecular vibrations is completely neglected. Their calculated peak position 2.4 eV for the hydrated electron is in surprisingly excellent agreement with the electronic transition energy $\langle\omega_0^1\rangle$, when there is no coupling to the intramolecular vibrations obtained from our

(31) Feng, D. F.; Kevan, L. *Chem. Rev.* **1980**, *80*, 1.
(32) Fueki, K.; Feng, D. F.; Kevan, L. *J. Am. Chem. Soc.* **1973**, *95*, 1398.
(33) Timidei, A.; Zerbi, G. *Z. Naturforsch.* **1970**, *25A*, 1729.
(34) Kuhn, L. P. *J. Am. Chem. Soc.* **1952**, *74*, 2492.
(35) Hallam, H. E. In *Structure of Water and Aqueous Solutions*; Luck, W. A. P., Ed.; Verlag Chemie: Weinheim, FRG, 1974; p 289.
(36) Narayana, M.; Kevan, L. *J. Am. Chem. Soc.* **1981**, *103*, 1618.
(37) Kevan, L. *J. Phys. Chem.* **1981**, *85*, 1628.
(38) Golden, S.; Tuttle, T. R., Jr. *J. Phys. Chem.* **1984**, *88*, 3781.
(39) Sprik, M.; Impey, R. W.; Klein, M. L. *J. Chem. Phys.* **1985**, *83*, 5802.
(40) Jonah, C. D.; Romero, C.; Rahman, A. *Chem. Phys. Lett.* **1986**, *123*, 209.
(41) Murphy, S. V.; Hibbert, D. B. *Radiat. Phys. Chem.* **1986**, *28*, 319.
(42) Rice, S. A.; Kevan, L. *J. Phys. Chem.* **1977**, *81*, 847.

theory. The parameter $\langle\omega_0^1\rangle$ obtained from our theory is 2.35 eV. This seems to be additional proof that the electron–solvent pseudopotential used in simulations is adequate. However, serious discrepancy appears in the interpretation of the band-broadening mechanisms of the absorption spectrum. Their results demonstrate that the band shape arises from inhomogeneous broadening of lines associated with transitions among the ground and first nine excited electronic states, where the transitions $s \rightarrow p_1$, $s \rightarrow p_2$, and $s \rightarrow p_3$ are the main contribution to the bandwidth.

On contrary, the picture that emerges from our results shows that the spectrum contains a Franck–Condon progression, where the bandwidth arises from broadening of vibrational lines due to dephasing, i.e., the distribution of the vibrational frequencies of the solvent environment resulting from the coupling of the intramolecular vibrations to the low-frequency modes of the H-bond bridges. Our results demonstrate that for water and methanol the transition occurs among the ground and first excited state and the static broadening due to the distribution of electron traps does not play any role in the process.

The surprising similarity between the simulated peak position and the parameter $\langle\omega_0^1\rangle$ in our model leads us to suggest that the main reason of the discrepancy in the interpretation of the bandwidth comes from the neglecting of the electron–vibron coupling in their simulations as a consequence of using rigid water. This conclusion seems to be supported by simulations of Barnett et al.[43] for the hydrated electron. They have used flexible water model with the RWK2-M water–water potential[44] and obtained better agreement with the experimental peak position (2.2 eV). However, the RWK2-M potential, although it reproduces some of the vibrational properties of water, predicts the wrong bandwidth of the ν_S(OH) mode.

Recently, improved potentials for water have been proposed.[45] The simulations of the solvated electron spectrum with the potentials which correctly reproduce the vibrational properties of the solvent would be valuable to determine the reason for the discrepancies between our conclusions and those of the simulation.

Jou and Freeman,[23] analyzing the band shape of water and alcohols, came to the conclusion that the low-energy side is due to the bound–bound transition and the band half-width is fitted by the statistical distribution of the traps. The high-energy side is a bound–continuum transition with the bandwidth containing the overlapping of the excited states and a continuum. We have shown that it is not necessary to assume that the experimentally observed asymmetry is due to two different mechanisms. The vibronic progression ν_t for water and ν_b for alcohols with the bands broadened due to the coupling with the intramolecular low-frequency stretching mode ν_σ of the hydrogen bridge OH···O reproduces the band shapes in the whole spectrum range.

4. Conclusions

Our model seems to generate the width and the asymmetry of the absorption spectra of the solvated electron in water and alcohols with fair accuracy. The visible spectra in water and methanol are ascribed to electrons in two different kinds of the traps—hydrogen bond OH oriented for water and dipole oriented for methanol toward electron.

The bandwidths arise from the combination of the vibronic bands due to the electron–torsional mode ν_t coupling for water and the electron–bending mode ν_b for methanol with the vibronic progression broadened by the coupling with the OH···O low-frequency stretching bridge mode ν_σ. The short-time dynamics probed by the spectral band shape is not affected by tunneling.

Registry No. Water, 7732-18-5; methanol, 67-56-1.

(43) Barnett, R. B.; Landman, U.; Nitzan, A. *J. Chem. Phys.* **1989**, *90*, 4413.
(44) Reimer, J. R.; Watts, R. O. *Chem. Phys.* **1984**, *85*, 83.
(45) Bopp, P. *Chem. Phys.* **1986**, *106*, 205.

Chemiluminescence Spectra of Thioformaldehyde and Selenoformaldehyde

R. J. Glinski,* C. D. Taylor, and H. R. Martin

Department of Chemistry, Tennessee Technological University, Cookeville, Tennessee 38505
(Received: August 14, 1990; In Final Form: April 1, 1991)

Moderate-resolution chemiluminescence spectra of CD_2S, CH_2S, and CH_2Se were obtained during the reaction of F_2 with methylated sulfur and selenium compounds at about 0.5 Torr of total pressure. Phosphorescence corresponding to the $\tilde{a}^3A_2 \rightarrow \tilde{X}^1A_1$ transition dominated all the spectra, and a trace of fluorescence, $\tilde{A}^1A_2 \rightarrow \tilde{X}^1A_1$, appeared only in the spectrum of CH_2Se. The ν_4 and ν_6 frequencies of the $\tilde{a}$ state of CD_2S are reported for the first time as 219.4 ± 5.0 and 572.6 ± 5.0 cm^{-1}, respectively. From the unusually shaped 4_1^1 band of CH_2S ($\tilde{a} \rightarrow \tilde{X}$) an improved value of the ν'_4 frequency was found to be 308 ± 30 cm^{-1}. The CH_2Se spectra yielded an improved measurement of the ν''_3 frequency, 860 ± 10 cm^{-1}, and new estimates of three other ground-state frequencies: ν''_2 = 1460 ± 30, ν''_4 = 906 ± 10, and ν''_6 = 914 ± 20 cm^{-1}. A spectrum of CH_2Te was sought in the reactions of CH_3TeCH_3 and $CH_3Te_2CH_3$ with F_2 but was not found; instead emission from TeF ($A^2\pi_i \rightarrow X^2\pi_i$) was observed.

Introduction

The spectroscopy of thioformaldehyde has received considerable attention recently.[1-3] With few exceptions the spectroscopic parameters of the $\tilde{a}$, $\tilde{A}$, and $\tilde{X}$ states are well determined.[4] The molecule remains an attractive candidate for spectroscopic and photophysical study because the $\tilde{a}$ and $\tilde{A}$ states lie relatively close together between 6000 and 7000 Å. By contrast, detailed spectroscopic study of selenoformaldehyde has just begun. Absorption[5] and laser-excitation[6-8] spectroscopies have partially characterized the $\tilde{a}^3A_2$ and $\tilde{A}^1A_2$ excited states of CH_2Se. The microwave spectrum has yielded rotational and geometric parameters of the ground state.[9,10] Except for estimates based on hot-band features

(1) Petersen, J. C.; Ramsay, D. A. *J. Mol. Spectrosc.* **1987**, *126*, 29.
(2) Suzuki, T.; Saito, S.; Hiroto, E. *J. Mol. Spectrosc.* **1985**, *111*, 54.
(3) Dixon, R. N.; Gunson, M. R. *Chem. Phys. Lett.* **1984**, *104*, 418.
(4) Clouthier, D. J.; Ramsay, D. A. *Annu. Rev. Phys. Chem.* **1983**, *34*, 31.
(5) Judge, R. H.; Moule, D. C. *J. Am. Chem. Soc.* **1984**, *106*, 5406.
(6) Clouthier, D. J.; Judge, R. H.; Moule, D. C. *Chem. Phys.* **1987**, *114*, 417.
(7) Judge, R. H.; Clouthier, D. J.; Moule, D. C. *J. Chem. Phys.* **1988**, *89*, 1807.
(8) Clouthier, D. J.; Judge, R. H.; Moule, D. C. *J. Mol. Spectrosc.* **1990**, *141*, 175.

0022-3654/91/2095-6159$02.50/0